Pergamon

Progress in Oceanography 49 (2001) 439–468

Progress in Oceanography

www.elsevier.com/locate/pocean

The pelagic ecosystem of the tropical Pacific Ocean: dynamic spatial modelling and biological consequences of ENSO

Patrick Lehodey

Oceanic Fisheries Programme, Secretariat of the Pacific Community, BP D5, 98 848 Noumea cedex, New Caledonia

Abstract

A feature of the central equatorial Pacific is a strong divergent equatorial upwelling called the cold tongue, which is favorable to the development of a large zonal band with high levels of primary production. Contiguous to the cold tongue, is the western Pacific warm pool, which is characterized by warmer water with lower levels of primary production. At the top of the food web, the tropical tunas are a major component of the pelagic ecosystem and have their maximum biomass in the warm pool. However, during ENSO (El Niño Southern Oscillation) events, variability is observed in both environmental factors and the spatial distribution of tuna. A Spatial Environmental Population Dynamics Model (SEPODYM) is used to assist in the analysis and interpretation of these fishery oceanographic observations. A modelling approach is described and applied to the population and fisheries of skipjack tuna, one of the top predator species with its greatest biomass in the tropical pelagic ecosystem. Environmental variables are used in the model for delineating the spawning area of skipjack, reproducing the transport of its larvae and juveniles, and simulating tuna forage. The forage production is deduced from a simple ecological transfer based on new primary production with biomass calculated as a single population. The model considers an interaction between predicted tuna density and forage density. A habitat index combining temperature preferences with forage distribution is used to constrain the movement of adult tuna. Results of the simulation allow realistic prediction of the large-scale distribution of the species. There is a remarkable out-of-phase pattern linked to ENSO between the western Pacific region and the cold tongue. This pattern is consistent with the observed movements of skipjack.

Contents

E-mail address: patrickl@spc.int (P. Lehodey).

0079-6611/01/$ - see front matter
PII: S0079-6611(01)00035-0

1. Introduction

Despite its low primary productivity rates, the western equatorial Pacific warm pool supplies the largest proportion of tuna catch (>1.5 million t year^{-1}) in the Pacific Ocean and contributes approximately 40% of the world's annual tuna catch. The global tuna catch is dominated by two tropical species, skipjack (*Katsuwonus pelamis*) and yellowfin (*Thunnus albacares*), which inhabit the surface mixed layer. These two species are amongst the top predators of the tropical pelagic ecosystem, and have the greatest biomass and the largest forage requirement (Kitchell, Boggs, He, & Walters, 1999). Given the link between primary production and fish production through the food web (Cushing, 1995), the antagonistic east–west distribution of primary production and tuna abundance initially appears paradoxical. In addition to these general features, the ENSO (El Niño Southern Oscillation) events, which are the main source of variability in the equatorial

Pacific, strongly affects both primary productivity (Murtugudde et al., 1999) and spatial distribution of tuna (Lehodey, Bertignac, Hampton, Lewis, & Picaut, 1997).

To explore the mechanisms that generate this fishery oceanographic situation and its variability, a spatial environmental population dynamics model (SEPODYM) is used. The model contains multi-gear and one or multi-species, with environmental and spatial components. Important features of the model are the use of an environmental-based habitat index to constrain the movement of tuna, and the development of a tuna forage sub-model. This sub-model was necessary because direct observations from sparse sampling are insufficient to describe the spatio-temporal distribution of tuna forage. In the initial version of the model (Bertignac, Lehodey, & Hampton, 1998) a constant mortality rate was used for the forage population (Lehodey et al., 1998). This up-dated version takes account of the interaction between predicted tuna density and forage density.

After a description of the model, the model is applied to the population and fisheries of skipjack tuna. Results are discussed in the context of the current understanding of equatorial oceanography in the Pacific Ocean.

2. Modelling approach in SEPODYM

All the spatial dynamic modelling of SEPODYM is based on a diffusion–advection equation in two horizontal dimensions. The use of diffusion models for simulating random dispersion of animal population is not a recent development and different applications are discussed in the literature (e.g. Skellam, 1973; Okubo 1980, 1986; Murray, 1993). However, in some cases animal populations show directional movement, and to account for this behavior, Okubo (1980, 1986) presented a derivation of the advection–diffusion equation, in which directional movements are described by the advective term of the equation. An extension of this approach has been used for the analysis of the movements of tagged tuna (Sibert, Hampton, Fournier, & Bills, 1999), and the treatment of the spatial dynamic component in SEPODYM uses the same mathematical formulation, except that the advective terms applied to this equation differ according to the simulated movements. For the movement of small forage organisms and tuna larvae and juveniles, the advective components in the two horizontal dimensions are oceanic currents, but for adult tuna they are habitat index gradients. The equations of transport in the two horizontal dimensions for forage and tuna populations are given in Bertignac et al. (1998) and Lehodey et al. (1998). The habitat index is a function of forage density and sea surface temperature. Sea surface temperature, oceanic currents, and primary production are also used in the model to delineate tuna spawning areas, transport larvae and juveniles, and simulate the tuna forage distribution.

The ‘basin model’ developed by MacCall (1990) proposed an approach to include spatial effects in a population dynamic model. As with SEPODYM, the model is based on the use of a habitat and a diffusion–advection equation. The habitat selection described by MacCall is density–dependent, i.e., the population size and local density influence the choice of habitat and hence the population’s distribution. In other terms, “as the density of individuals increases in a habitat, realized suitability decreases from the basic level”. The approach is different in SEPODYM, although the interaction between density of tuna and density of forage is also considered by coupling tuna forage and tuna population sub-models. The contribution of tuna predation to the forage mortality is proportional to the density (biomass) of tuna. Therefore, an increasing density

of tuna increases the forage mortality, and if there is no additional supply of forage, decreases the habitat index value. Since the movement of tuna is based on the gradient of the index, tuna will start to leave the zone when forage is no longer abundant enough to support the local tuna population density. On the other hand, tuna will continue to concentrate if the index value remains higher than in neighboring zones. This approach seems appropriate for reproducing tuna behavior, particularly the frequent huge aggregations of tuna feeding on large patches of prey organisms.

3. The forage model

3.1. Theoretical bases

A basic difference between pelagic and terrestrial ecosystems is that the size of the food particles is a primary determinant of food web structure in the open sea (Isaacs, 1977). From extensive observations of marine pelagic communities, Sheldon, Prakash, and Sutcliffe (1972) found that particle concentrations over a wide range (from phytoplankton to whales) are relatively uniform when data are grouped in logarithmic size intervals. Following this work, numerous studies have attempted to characterize the pelagic ecosystem as a function of organism size, leading to the concept of biomass size spectra (Platt, 1985; Dickie, Kerr, & Schwinghamer, 1987). There are many studies that have described empirical relationships between body size of aquatic organisms and other attributes, such as sizes of prey and sizes of their predators, size and metabolism (Borgmann, 1982; Platt, 1985), size and population generation time (Sheldon et al., 1972), size and production or biomass (Rodriguez & Mullin, 1986; Boudreau & Dickie 1989, 1992), and more recently, size and nitrogen isotopic composition (δ^{15}N) of organisms (France, Chandler, & Peters, 1998), which is proposed as a good indicator of the trophic level. Supporting the concept of biomass size spectra, the evaluation of biomass of the major components of oceanic epipelagic (0–200 m) communities conducted by Shushkina, Vinogradov, Sheberstov, Nezlin, and Gagarin (1996), and Shushkina, Vinogradov, Lebedeva, and Anokhina (1997) suggest that a simple decreasing function could describe the mean ecological transfer of biomass through successive compartments of the ecosystem, regardless of the level of primary production of the oceanic region (Fig. 1). These findings provide important theoretical bases for model development to describe biomass or energetic flow through aquatic ecosystems (e.g. Kerr, 1974; Sheldon, Sutcliffe, & Paranjape, 1977; Silvert & Platt, 1978; Cousins, 1985; Borgmann, 1987; Boudreau & Dickie, 1989). These numerous examples suggest there is a trophic continuum in the pelagic ecosystem with a size-related time-scale.

3.2. Considering forage as a single population

Instead of developing a detailed explicit food web through the whole pelagic ecosystem, which is a complex and very long task, the tuna forage is considered as a single population. Since all the organisms of a same cohort have the same age, it is immaterial whether the cohorts are of the same species or not (Allen, 1971). The dynamic of the forage population is simply described by a continuous recruitment S and a constant mortality rate λ as in Lehodey et al. (1998). The recruitment consists of new organisms entering into the forage population at a given time. Since

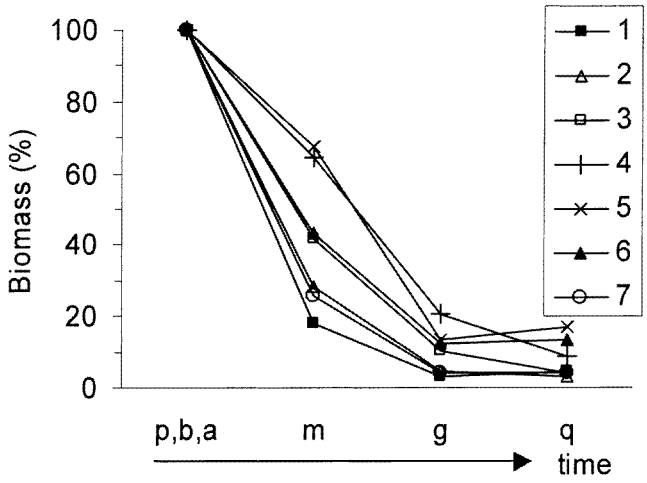

Fig. 1. Percent biomass relative to the phytoplankton biomass of principal components of planktonic pelagic communities of the tropical Pacific Ocean (40°N–40°S), with different productivity in the upper 200 m layer. Calculated from the work carried out by Shushkina et al. (1996, 1997). (p,b,a) phytoplankton+bacteria+protozoa, (m) small mesoplankton ≤3 mm, (g) large mesoplankton >3 mm and (q) macroplankton >30 mm. Tropical Pacific Ocean regions: 1 hypertrophic; 2,3 eutrophic; 4,5 mesotrophic; 6 oligotrophic; 7 ultraoligotrophic.

the tuna forage does not include all the organisms developing along the food chain from the primary level, the time of recruitment (T_r) allows to select an adequate spectrum of organisms of the forage. In other terms, the time T_r is the minimum time necessary for the development of organisms between their 'birth' and 'recruitment' into the forage population.

In a classical fish population model, the origin of the recruitment is the biomass of spawning adults. In the case of the forage population, it is the development of a new primary biomass over a period of time (new primary production) that allows the development of a new cohort of many different organisms, a fraction of which will be recruited after a time T_r into the forage population. The amount of the fraction transferred depends on an ecological transfer coefficient. To follow the energy transfer from primary production to forage, the nitrogen unit of primary production is also used for the forage population. Therefore, the forage biomass is the accumulated quantity of nitrogen in the population. There is no growth function for the forage population, but an appropriate coefficient is used to convert this quantity of nitrogen to wet weight.

Since the cohorts are identical in their growth and mortality, it is not necessary to consider effects that result from the existence of more than one cohort, if the recruitment is assumed constant (Allen, 1971). This is illustrated in Fig. 2 where the evolution in time of a single cohort is presented. Because of the constant coefficient λ, a given source term will decrease exponentially, and in the case of a constant source, the biomass (F) would tend towards an equilibrium level (S/λ). The total biomass integral by time of a single cohort is equal to the total biomass of the population of successive and identical cohorts. The exponential mortality model used, with a constant instantaneous rate, implies a ratio of production/biomass equal to the instantaneous mortality rate (1).

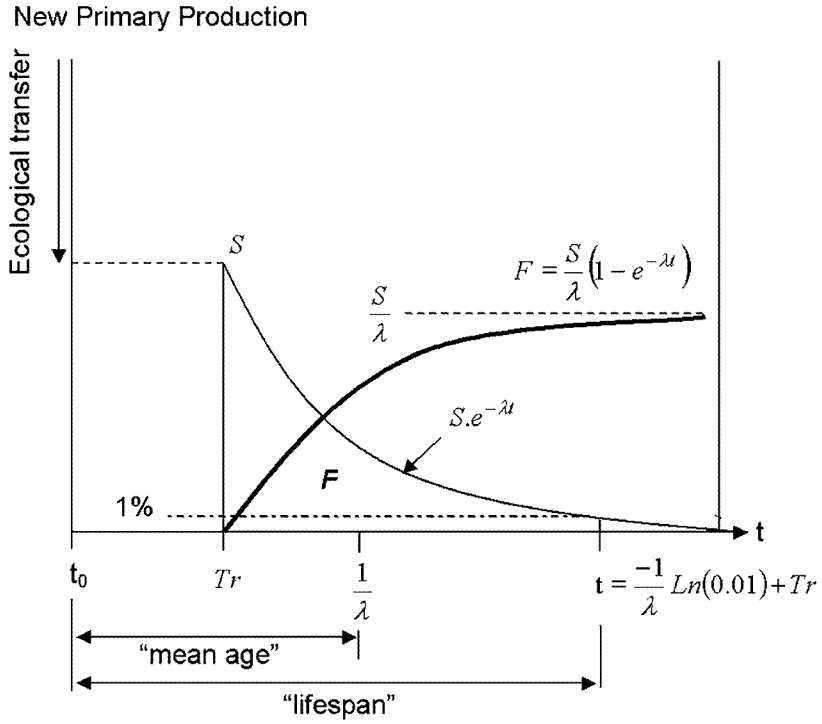

Fig. 2. Transfer with time of primary production to forage according to the model (S is assumed constant). The thin curve describes the evolution in time of a single source of primary production. The thick curve gives the total forage population, i.e., the sum of the shaded area.

$$\lambda = \frac{F'}{F} \tag{1}$$

Therefore, in an equilibrium situation, the biomass $F \sim S/\lambda$ and the production $F' = S$.

3.3. Characterizing the forage population with λ and T_r

Assuming that the recruitment S is constant and continuous allows defining a 'mean age' to the forage population (Fig. 2). If T_r is at time 0 of the forage population, the sum of the products $t.S_t$ is:

$$\int_0^\infty t.S \, dt = S \int_0^\infty t e^{-\lambda t} \, dt = \frac{S}{\lambda^2} \tag{2}$$

Since the forage population is S/λ, the mean time spent in the forage population is S/λ^2 divided by S/λ, or $1/\lambda$. Adding T_r to $1/\lambda$ gives the 'mean age' of the forage population since the origin of the cohort, i.e., the time when the new primary production appears. Specifically, it is a biomass-weighted mean age because the forage population is expressed in units of biomass. The

mean age can be assimilated to the interval between one generation and the next, such as a mean generation time or turnover time (the mean time taken for the biomass of the population to be replaced by fresh production). It is also possible to define the maximum life span of organisms within the forage population as the time necessary to see the population reduced by a determined level (e.g., for 99%, $t=-1/\lambda$ Ln(0.01)+T_r). Therefore, λ and T_r which characterize F can be estimated using biological characteristics of key-species representative of the forage population.

3.4. Ecological transfer toward forage production

To determine a realistic value for the ecological transfer, independent estimations of the efficiency coefficient of ecological transfer from primary to secondary levels of the pelagic food web have been derived from a literature search. For example, Iverson (1990) calculated that nitrogen transfer efficiency (E) was a constant 0.04 in oceanic and coastal environments with an average 2.5 trophic transfers from phytoplankton to carnivorous fish and squids (typically tuna prey species). In other words, 4% of the new primary production (or nitrogen) is transferred to the forage production (Fig. 2). (In Lehodey et al. (1998), the transfer from new primary production to forage production was considered to decrease continuously during T_r, by using an exponential function with a loss rate $m_r=-\ln(E)/T_r$.)

During the period T_r, the cohort of organisms that is developing from a new contribution of primary production is also under the influence of the motion of water masses. As a consequence, the transport model must be applied during this period to the fraction of nitrogen content of the primary production that is transferred toward the forage population.

3.5. Application to tuna forage

Tunas are known to be opportunistic predators feeding upon three major groups of prey: fish, squids and crustaceans. Sizes of the prey items range from a few millimeters (small euphausiids and amphipods) to several centimeters (squids, small fish, shrimps). A prey–predator size dependent selectivity has been expressed as a correlation between prey item size and the size between their gill rakers (Magnuson & Heitz, 1971). Consequently, the proportions of the three major groups of prey in the tuna diet vary according to the size of the tuna and the diverse faunal assemblage occurring in different oceanic areas (Matsumoto, Skillman, & Dizon, 1984). The result is a large spectrum of prey species and prey sizes that is difficult to incorporate into an explicit trophic model. The integrated tuna forage model described above appears more suitable as a means of modelling tuna forage.

Biological characteristics of the main tuna prey species or group of species can be found in the literature. For tropical cephalopod species (Jackson & Choat, 1992), size-at-age data suggests a rapid growth, with achievement of full size in less than 200d and short life span (less than one year). In the eastern Pacific, a key prey species of skipjack appears to be the red crab, *Pleuroncodes planipes* (Forsbergh, 1980). Its larval phase is about 130d (five zoeal stages) and postlarval phase (2 to 6 mm) about 4 or 6 months, with individuals reaching sexual maturity (at ~16 mm) in about 1 year (Gomez-Gutierrez & Sanchez-Ortiz, 1997). In the western Pacific, schools of skipjack and yellowfin regularly feed on high concentrations of the zooplanktivore oceanic anchovy, *Encrasicholina punctifer* (Hida, 1973), a species with a short life cycle (less than 1

year), a rapid growth and an age at maturity of 3–4 months (Dalzell, 1993). Euphausiids are also frequently found in skipjack stomach contents, and their life span appears to be ~1 year (10–15 months) with sexual maturity at 8–10 months (Roger, 1971).

A mean age of 120d was chosen since it is the age at maturity for the oceanic anchovy, a predominant prey of skipjack in the warm pool. A value of 60 d is assigned for T_r. At this age, the juvenile skipjack that are frequently found in the stomachs of adults are 10–15 cm. These parameter values lead to a maximum life span of 336 d. Although these values may need to be more accurately refined, they appear to be a reasonable characterisation of tuna forage according to biological studies of typical prey species.

4. The tuna population model

4.1. Tuna ecology and habitat

Tuna are amongst the most highly specialized fishes with regard to sustained, high levels of locomotory activity. They swim continuously to counterbalance their negative buoyancy, and are able to travel hundreds of miles. This high expenditure of energy enables them to move quickly through their environment in search of their food, from which they require correspondingly large energy returns. This strategy has resulted in morphological and physiological adaptations, particularly associated with their thermoregulation and high efficiency in oxygen extraction. Consequently, these two major features of the oceanic environment, ambient temperature and dissolved oxygen concentration, are believed to influence tuna behavior strongly (Brill, 1994). The relationships between tuna physiology and ambient temperature and oxygen concentration have been studied in laboratory experiments, by in situ tracking experiments and by comparisons between catch statistics and oceanographic conditions (e.g. see reviews in Sharp & Dizon, 1978; Forsbergh, 1980; Matsumoto et al., 1984; Brill, 1994). Sea surface temperature and oxygen concentration have been used to define large-scale limits to potential tuna habitat (Barkley, Neill, & Gooding, 1978). The distribution of tuna forage within this potential habitat probably has the major influence on tuna distribution. Surface tuna like skipjack and yellowfin feed visually mainly during the daylight hours. So, water clarity is also likely to influence their distribution. Therefore, the habitat of surface tuna could be defined in general terms as water masses with a combination of suitable temperature and sufficient oxygen concentration (varying according to species and life stage), high forage biomass and also clear water.

4.2. Description and parameterization

Tuna population dynamics have been described in Bertignac et al. (1998) and all the symbols used in the model are in Appendix A. The total level of recruitment is scaled to obtain a standing stock at equilibrium in agreement with independent estimations. Tuna stock–recruitment relationships are poorly known and recruitment is usually assumed to be independent of the adult population density, mainly because tuna have very high fecundity and spawn throughout the year over a large area. Therefore, the present simulation does not assume any stock–recruitment relationship, but the spatial distribution of recruits is environmentally constrained by the processes occurring

in the pre-recruitment period. First, the spawning area is limited by the presence of mature tuna and by sea surface temperatures (SST) above a limiting value. This latter condition is supported by the high correlation found between SST and occurrence of reproductively-active tropical tuna (Schaefer, 1998). Thereafter, during a short period of development (4 months), larvae and juveniles are passively transported by the currents. Following this period, young tuna become autonomous and move according to the same gradient of habitat index as the adults. Finally, once they reach the age of recruitment they are considered the first age class of the exploitable fraction of the population. The parameterization of the model is summarized in Table 1.

4.3. Habitat index

The habitat index combines the spatial distribution of forage with a temperature function defined for each tuna species according to our knowledge of their physiology and behavior. A function with a normal distribution is used for temperature and a linear function for forage, with both functions being scaled between 0 and 1 (Fig. 3). Therefore, for each cell of indices i, j, at time t, the habitat index $H_{i,j,t}$ is calculated as:

$$H_{i,j,t}=I_{i,j,t}\phi_{\mathrm{sp}}(\theta_{i,j,t}) \tag{3}$$

where $I_{i,j,t}$ is the forage density reduced to a range of 0 to 1 using Eq. (4),

$$I_{i,j,t}=\frac{1}{F_{\max}}F_{i,j,t} \tag{4}$$

and $\phi_{\mathrm{sp}}(\theta_{i,j,t})$ is the temperature function of the species sp defined as:

$$\phi_{\mathrm{sp}}(\theta_{i,j,t})=\frac{\gamma}{\sigma_{\mathrm{sp}}\sqrt{2\pi}}\exp\left[\frac{-(\theta_{i,j,t}-\theta_{\mathrm{sp}})^2}{2\sigma_{\mathrm{sp}}^2}\right] \tag{5}$$

where $\theta_{i,j,t}$ is the SST in cell of indices i,j,t, γ is a constant, and θ_{sp} and σ_{sp} are respectively the optimal temperature and its standard deviation for species sp. The habitat functions for skipjack are presented in Fig. 3.

5. Coupling forage and tuna models

In a previous version (Bertignac et al., 1998; Lehodey et al., 1998), the forage mortality caused by the tuna species was assumed to be included in the total mortality λ. However, the use of the predicted distribution of forage to constrain the movement of tunas without considering the feedback effect of tuna density distribution has implicit hypotheses. Either the forage mortality resulting from the tuna predation is assumed very low and relatively negligible to the total mortality of forage, or the predators present an 'ideal distribution'. In this latter case, the different predator species would have a natural ideal distribution, such that the total forage mortality by these species would be the same everywhere and equal to λ. This hypothetical situation presents an analogy with the 'ideal free distribution' proposed by Fretwell and Lucas (1970) and Fretwell

Table 1
Main biological parameters used in the simulation model for skipjack

Parameter			References
Number of age classes	36 (months)		
Age and growth	L_∞=70 (cm) K=1.33 (yr^{-1}) T_0=0 (yr)	(von Bertalanffy growth model)	Hampton (unpublished data)
Length-weight	a=8.6388 E-6 b=3.2174	$w=aL^b$	OFP (unpublished data)
Reproduction and recruitment			
Age of 1st maturity	9 (months)		
SST limit for reproduction	26°C		Schaefer (1998)
Recruitment (in number) by cell of 1° square	300,000		
Larvae–juvenile phase (passive transport)	4 (months)		
Natural mortality	Immature: 0.2 ($month^{-1}$) Adult: 0.2 ($month^{-1}$)		Hampton (unpublished data)
Initial stock biomass (equilibrium)	2–2,500,000 (t)	in the western Pacific 20°N–20°S, up to 150°W	Kleiber, Argue, and Kearney (1987)
Forage	E=0.04 T_r=60 (d) λ=1/60 (d^{-1}) r=0.1		
Habitat	θ_{sp}=30 (°C)		
Temperature function	σ_{sp}=2 (°C) γ_{sp}=5		
Forage function	F_{max}=10 (mmol N m^{-2})		
Movement			
Diffusion of skipjack (D)	320 (Nm^2 d^{-1})		
Diffusion of forage/larvae/juveniles (ρ)	250 (Nm^2 d^{-1})		
Advection coefficient (χ_0)	4000 (Nm d^{-1})[a]		

[a] Typically, 80% of the gradient of index values are in the range [−0.02, 0.02], i.e. corresponding to advective movements between 0 and 80 Nm d^{-1} (Nm=nautical miles).

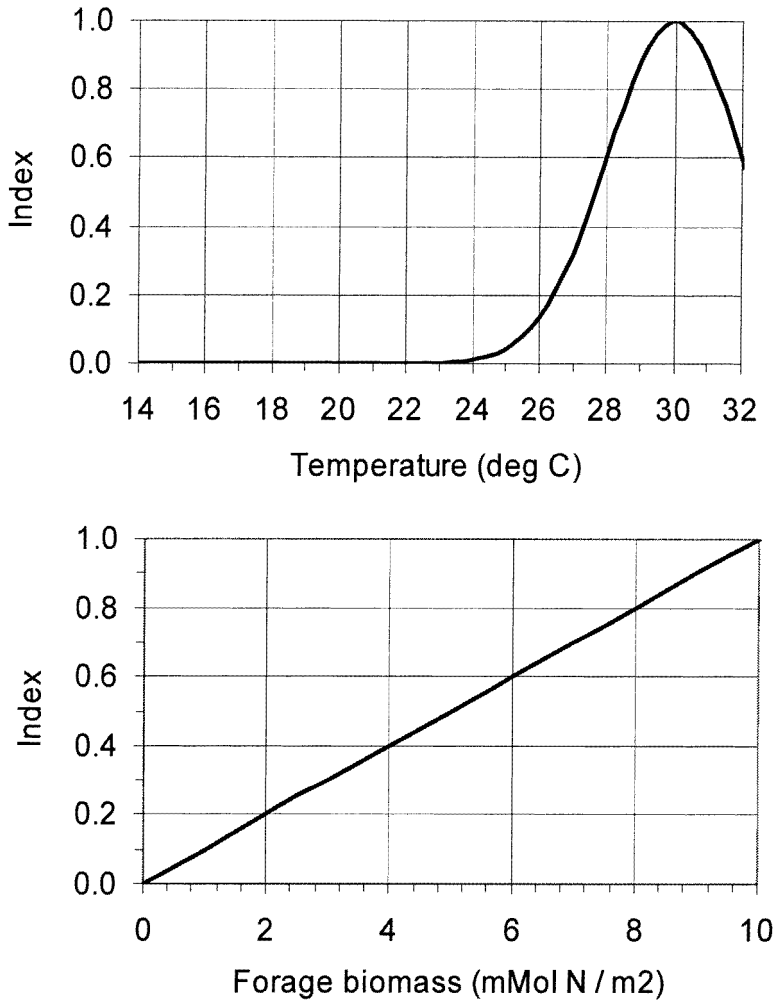

Fig. 3. Temperature and forage functions used to define the skipjack habitat in the present SEPODYM simulation.

(1972) for the density dependent habitat selection theory, whereby individuals differentially occupy available habitats so that realized 'suitability' is equal for all occupied habitats.

To have more realistic predator-prey interactions, and eventually to test these hypotheses, the forage mortality has to be dependent on the tuna density. The approach used was to calculate and apply first a specific local mortality $\omega_{i,j,t}$ resulting from the food requirements of tuna population described in the model, then a mean residual mortality λ' which is the difference between the total mortality λ and the mean specific mortality $\overline{\omega_t}$ over the area occupied by tuna (6). Therefore, the total forage biomass over the whole area remains equal to the total forage biomass calculated in the case of a constant λ, but the spatial distribution linking the density of tuna may be different. Eqs. (6)–(10) are given for one predator species but the extension to several predator species is straightforward.

$$\lambda'_t = \lambda - \overline{\omega_t} \tag{6}$$

To obtain ω, the forage required (F_R) by the tuna species is calculated by knowing a daily food ration r (eventually by age class a) relative to its weight w (7). The specific mortality rate is defined as the ratio of the forage biomass requirement (F_R) for the species to the forage biomass available F (8). A conversion factor (c_4) is used to express the forage biomass in a similar unit as F_R (see Appendix A).

$$F_{Ri,j,t}=\sum(N_{i,j,t,a}.w_a.r_a) \tag{7}$$

$$\omega_{i,j,t}=\frac{F_{R_{i,j,t}}}{F_{i,j,t}.c_4} \tag{8}$$

The mean specific mortality over the whole area occupied by the predator species is:

$$\overline{\omega_t}=\frac{\sum F_{R_t}}{\sum F_t} \tag{9}$$

It is possible to define a consumption coefficient Q as the ratio of F_R to the forage production. Thus, Eq. (8) is equivalent to:

$$\omega_{i,j,t}=\frac{Q_{i,j,t},S_{i,j,t}}{F_{i,j,t}} \tag{10}$$

A value of $Q>1$ (or a negative value of λ') indicates that forage production is lower than tuna F_R, i.e., that mortality cause just by tuna predation is greater than total mortality λ ($Q=F_R/S=\omega/\lambda>1$) . In this case, the parameterization or the hypotheses of the model should be revised.

6. Numerical resolution and simulation

Extensive description of the mathematical model used for the transport can be found in Sibert and Fournier (1994), Bills and Sibert (1997) and Sibert et al. (1999). The differential equations are numerically solved by finite-difference techniques using a network of regularly spaced grid points and a discrete time step. The upwind differencing scheme (Press, Teukolsky, Vetterling, & Flannery, 1992) is used for approximating the first derivatives in the advection terms.

In this simulation, the spatial resolution is one degree square and the time step is 5 d. The input data set (primary production, currents, temperature) was provided by a coupled run between a three dimensional OGCM (Blanke & Delecluse, 1993) developed at the LODYC (Laboratoire d'Océanographie Dynamique et de Climatologie) with a biogeochemical model (Stoens, Menkes, Dandonneau, & Memery, 1998; Stoens et al., 1999). The predicted new primary production (P) was integrated within the euphotic zone and the predicted currents averaged on the same layer. A 'spin-up' of several years is used to build the forage and tuna populations, then fisheries are started and predictions are recorded.

Three different fishing gears are described: purse-seine, pole-and-line and a group of mixed domestic gears from the Philippines and Indonesia. A total of nine fleets are represented (Table 2), each with separate catchability coefficients. An age-based selectivity function is used for each gear (Fig. 4). The fishing effort of each fleet varies by month and in space, with a one degree square resolution except for the Philippine and Indonesia fleets that provide data aggregated by five degree square, and year. The recruitment (or spawning) is adjusted, so that the stock biomass estimates are roughly equal to those obtained independently from other studies. The catchability coefficients are then scaled to obtain estimated catches at the same level as observed catches. Results of the simulation are compared to observed fishing data by fleets, such as total monthly catch, spatial distribution of catch, and distribution of length frequencies.

7. ENSO variability and primary production in the tropical Pacific

Since the results of the simulation are strongly dependent on the environmental factors that constrain the model, a brief overview of the oceanography of the tropical Pacific Ocean is presented to help in interpretation.

The warm waters in the surface layer of the western equatorial Pacific (the warm pool) have a temperature $>28°C$ year-round, inducing an atmospheric convection connected to the colder eastern Pacific Ocean through the Walker circulation. The intense atmospheric convection associated with the warm pool results in a large excess of precipitation compared to evaporation. Consequently, the warm pool contrasts with the central equatorial water masses by having warmer waters of relatively lower salinities. In this warm pool, the balance between precipitation and entrainment of subsurface saltier water results in haline stratification: a structure called the barrier layer (Lukas & Lindström, 1991) appears when the isohaline layer is shallower than the isothermal layer. A major consequence of this haline stratification is the inhibition of the downward penetration of energy generated by the westerly wind bursts that occur in the western Pacific. This results in a trapping of westerly wind burst momentum in the surface layer (Vialard & Delecluse,

Table 2
Observed average fishing effort and skipjack catch in tonnes (for 1993–1994) by fleet, and the estimated catchability coefficient

Fleet	Fishing effort (days)	Catch (t)	Catchability
Eastern Pacific US purse, seine	17,939	65,575	0.022
Japanese purse, seine	6332	112,811	0.106
Korean purse, seine	4743	115,057	0.280
Taiwanese purse, seine	10,152	125,487	0.066
Western Pacific US purse, seine	8878	147,622	0.029
Japanese pole-and-line	4187	33,895	0.036
Solomon pole-and-line	6789	18,624	0.018
Fiji pole-and-line	1378	3488	0.015
Domestic Philippine–Indonesia	23,360	202,842	0.032
Total	83,756	825,401	

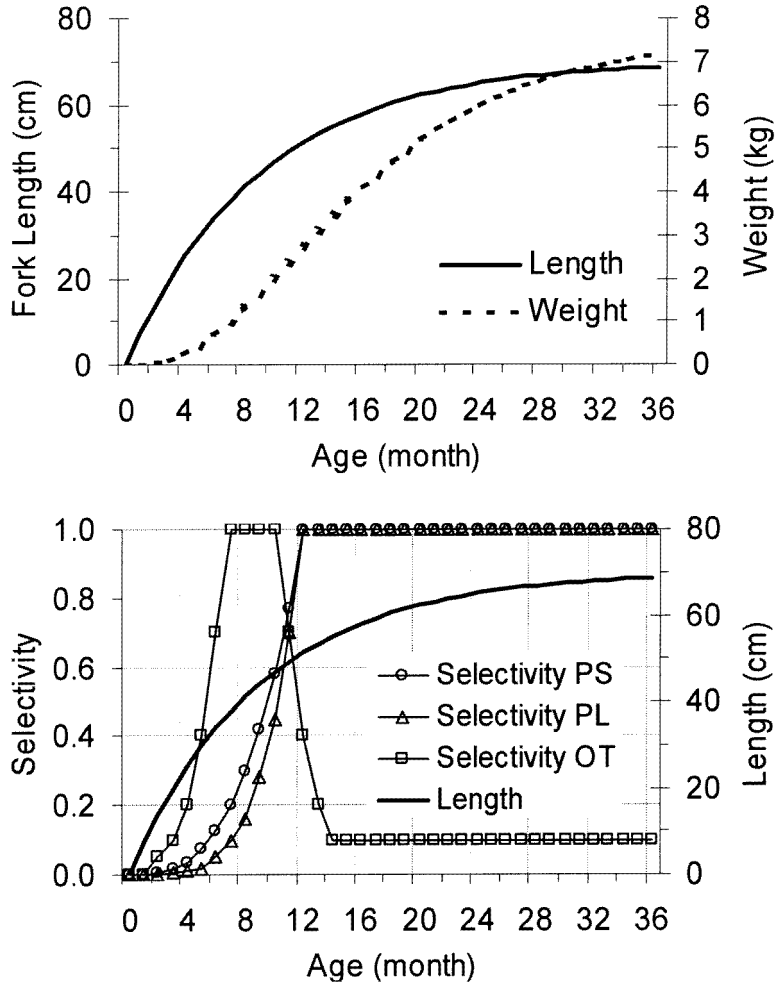

Fig. 4. Growth in length-at-age and weight-at-age for skipjack, and selectivity function used for skipjack in the present SEPODYM simulation.

1998), giving rise to strong eastward equatorial currents. This zonal advection of the surface layer affects the extent of the warm pool and appears to be a major process in the development of El Niño events (MacPhaden & Picaut, 1990; Delcroix, Eldin, & Radenac, 1992; Picaut & Delcroix, 1995; Picaut, Masia, & Du Penhoat, 1997; Delcroix, 1998).

Contiguous to the warm pool in the central equatorial Pacific is an equatorial divergence, along which relatively cold and nutrient-rich water upwells. This equatorial divergence is within the mean westward zonal flow of the South Equatorial Current (SEC). The intermittent eastward surface flow in the western Pacific generated by westerly wind bursts encounters this westward advection and induces a convergence zone along the eastern edge of the warm pool, which is characterized by a salinity front or, more approximately, by the 29°C or 28.5°C isotherm. In the average situation, the convergence zone oscillates around 180°, but it shows spectacular zonal displacements in association with ENSO signals.

The biological consequence of the equatorial upwelling is to generate a large zonal band in which there is high primary production, frequently called the cold tongue, and which contrasts with both the generally low primary productive waters of the western Pacific warm pool and the subtropical gyres to the north and south, where primary production rates are the lowest in the Pacific Ocean (Longhurst, Sathyendranath, Platt, & Caverhill, 1995). However, the primary productivity in the tropical Pacific is strongly influenced by ENSO events.

During El Niño phases, wind stresses in the western Pacific are stronger, and the barrier layer either dissipates or shifts eastward (Vialard & Delecluse, 1998). In the absence of the barrier layer, the wind stress can drive the mixed layer deeper, which favours an increase in primary production in the region; this is clearly evident in Fig. 5. This figure represents composite images of phytoplankton pigment concentration derived from CZCS satellite data for the 1982–83 ENSO and SeaWiFS satellite data for the most recent event of 1997–2000. They reproduce the contrasting situations of El Niño and La Niña events.

During La Niña, a rich (mesotrophic) chlorophyll cold tongue is clearly visible, extending as far west as 160°E, while the warm pool from Philippines to 160°E is typically in a low primary productivity situation (oligo- to ultra-oligotrophic). During El Niño the cold tongue retreats east of 180°. With this eastward movement, warm waters and associated atmospheric convective zone extend to the central Pacific. This displacement is associated with a decrease in equatorial

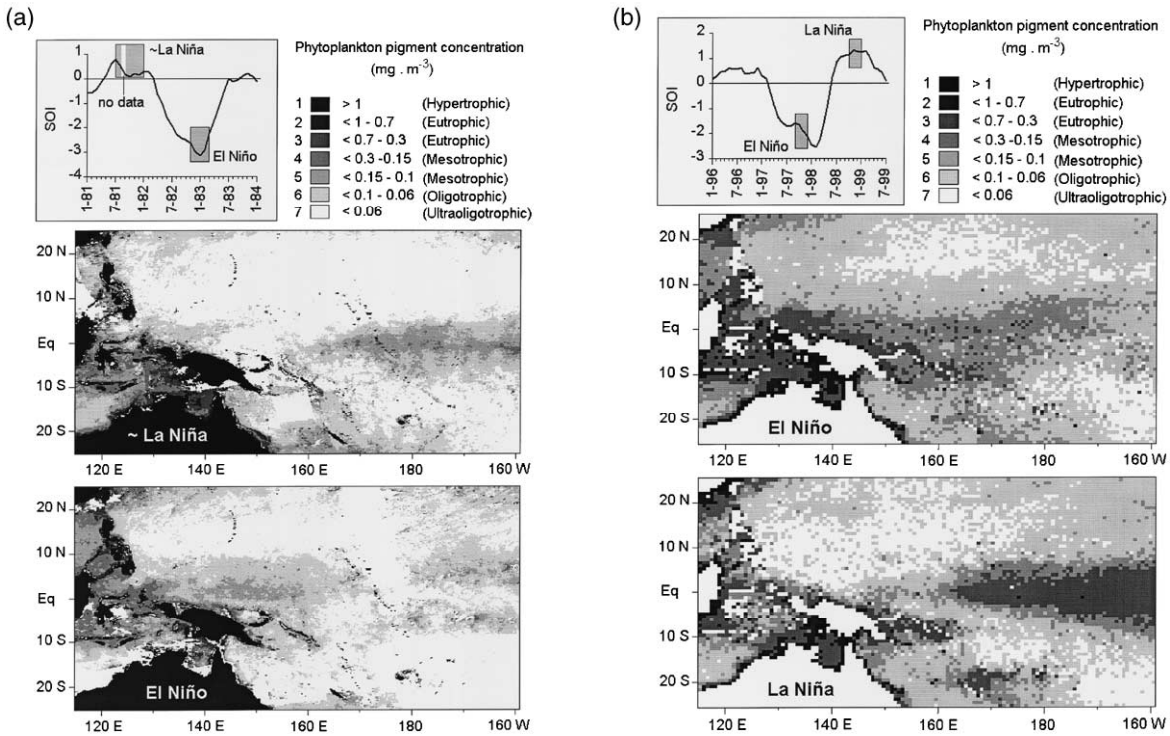

Fig. 5. Impact of the ENSO signal on primary productivity in the western and central equatorial Pacific. Composite images from the CZCS and SeaWiFS satellite data for two opposite phases of ENSO identified in the upper box (classification follows that defined by Shushkina et al., 1997).

upwelling and primary production. During the same period, the oceanic region between the Philippines and 160°E–180° shows an enrichment in phytoplankton biomass and coastal upwelling is well developed along the north coast of Papua New Guinea. In addition to this general pattern, specific events can occur such as the development of the large phytoplankton bloom, which was observed along the Equator near 165°E (Murtugudde et al., 1999) before the last El Niño abruptly ended in mid-1998. The development of this bloom appeared to coincide with the disappearance of the barrier layer and the appearance of easterly wind-anomalies (Murtugudde et al., 1999).

8. Limitations

The simulated primary production used in the present application of SEPODYM reproduces the ENSO variability in the equatorial Pacific with reasonable agreement between observed and predicted data (Stoens et al., 1999). However, there are several limitations:

1. The simulated nitrate is relaxed to Levitus climatology on the four east, west, north and south boundaries, so that it is difficult to evaluate the change of productivity linked to ENSO in the far western (115°–130°E) Pacific with this simulation.
2. The coastal upwelling along the coast of Peru and Chile are not fully included since the eastern grid boundary is 80°W, and
3. Primary production is likely to be overestimated in the mesotrophic regions where modelled chlorophyll was generally higher than the observations (Stoens et al., 1999).

9. Results

9.1. Skipjack habitat

Many authors have used SST for delimiting skipjack distributions and the optimum ranges for commercial fishing. Their temperature range is normally between 20° and 30°C, but occasional catches do come from waters $<$20°C, with a clear temperature limit of 15°C. The largest catch comes from equatorial waters where SST is $>$28°C. Therefore, the temperature function for skipjack shown in Fig. 3 is considered to be representative of the temperature preference of this species. Such a function should be sufficient to consider the seasonal movement of skipjack associated with the warming of sub-tropical surface water during summer (Fig. 6a), and leading to the seasonal development of fisheries off the coasts of Japan in the northern hemisphere, and Australia/New Zealand in the southern hemisphere. Indeed, by combining the temperature and forage effects into a habitat index, the attractiveness of the temperate regions in summer increases rapidly with temperature because the availability of forage in these regions is high (Bertignac et al., 1998).

The overall pattern of the simulated forage distribution (Fig. 6b) has been previously described (Lehodey et al., 1998). Its availability is probably overestimated along the southern boundary of the central equatorial upwelling, because here primary production is overestimated. Consequently,

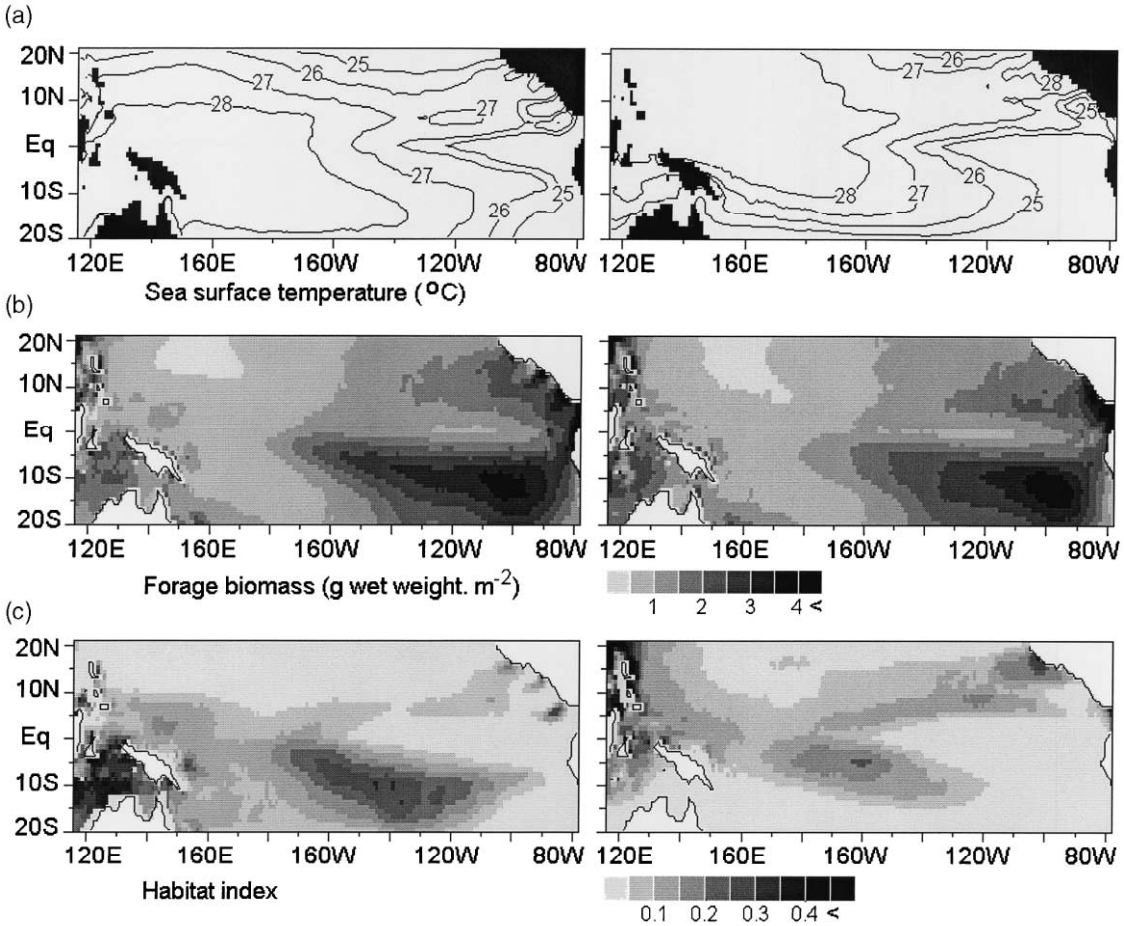

Fig. 6. Spatial distributions of SST, predicted forage and habitat for a mean situation in the 1st and 3rd quarter (1st quarter is the average of the 1st quarters of 1993, 1994 and 1995; 3rd quarter is the average of the 3rd quarters of 1992, 1993, and 1994).

when SST and forage effects are combined (Fig. 6c), this region shows maximum habitat index values that are also probably too high. Nevertheless, the spatial distribution of habitat has high values in the Philippine–Indonesia region, the equatorial western central Pacific, and the northeastern equatorial Pacific along a latitudinal band centered on 5°N. The seasonal signal with an extension to higher latitudes in summer is also clearly visible. These features correspond quite well with the zones of high skipjack abundance and fisheries. Moreover, ENSO variability appears to have large repercussions on the dynamical distribution.

As for the primary production, a zonal displacement is observed in association with the ENSO oscillation, though of lower amplitude. When El Niño develops, the cold tongue retreats eastward and decreases in intensity much more rapidly than the bands of forage, which leads to a maximum decoupling when El Niño is fully developed. When oceanographic conditions return to a normal situation, the intensity of the new primary production in the cold tongue increases while its westward extension starts again. On the other hand, the biomass of tuna forage continues to decrease

in the central Pacific, due to the time lag of several months between primary production and tuna forage.

As the ENSO variability of forage is combined with the zonal displacement of the warm waters of the warm pool, an interesting out-of-phase pattern appears in the habitat distribution between the western and central equatorial Pacific. During the El Niño phase of 1994, a zone of rich habitat occurred in the central equatorial Pacific and was exploited mainly by the U.S. purse seine fleet (Fig. 7). The eastward displacement of this favorable habitat zone was consistent with the observed movement of tagged skipjack and high skipjack tuna catch rates from this region (Lehodey et al., 1997). When oceanographic conditions return to a more normal situation, the fishing fleets moved westward and continued to make good catches. The predicted habitat from the model has effectively increased in this western region. However, habitat index values remain the highest in the central Pacific region south of equator, where the predicted forage is likely to have been overestimated.

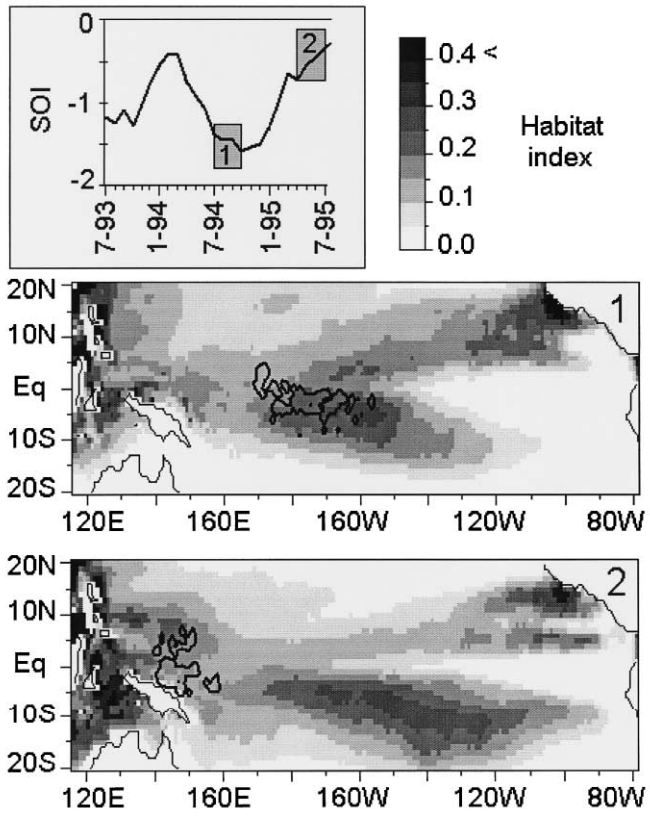

Fig. 7. Predicted skipjack habitat for two opposite phases of ENSO (identified in the upper box) corresponding to the development of a medium amplitude El Niño oscillation in 1994–95. The black iso-contours delimiting high catch levels of the US purse-seine fleet (above 40 t per degree square and quarter) are superimposed.

9.2. Skipjack population and stock

The spawning criterion of a SST >26°C is obviously favorable for good recruitment in the western central Pacific Ocean (WCPO), and the overall distribution of larvae and juveniles (Fig. 8a) reproduces the SST distribution. Distribution of larval skipjack is known from net tows by Japanese research vessels (Ueyanagi, 1969; Nishikawa, Honma, Ueyanagi, & Kikawa, 1985; Forsbergh, 1980). The simulated distribution of larvae and juvenile skipjack agrees well with these observations. In particular, the simulation reproduces their wide distribution in the WCPO, with an abrupt narrowing toward the equator at about 145°W.

Mori (1972) investigated the distribution of young skipjack. He noted they were more widely distributed than larvae and juveniles. He suggested that the young skipjack leave the nursery grounds when they have reached a length of ~30 cm. In the model, this behavior corresponds to

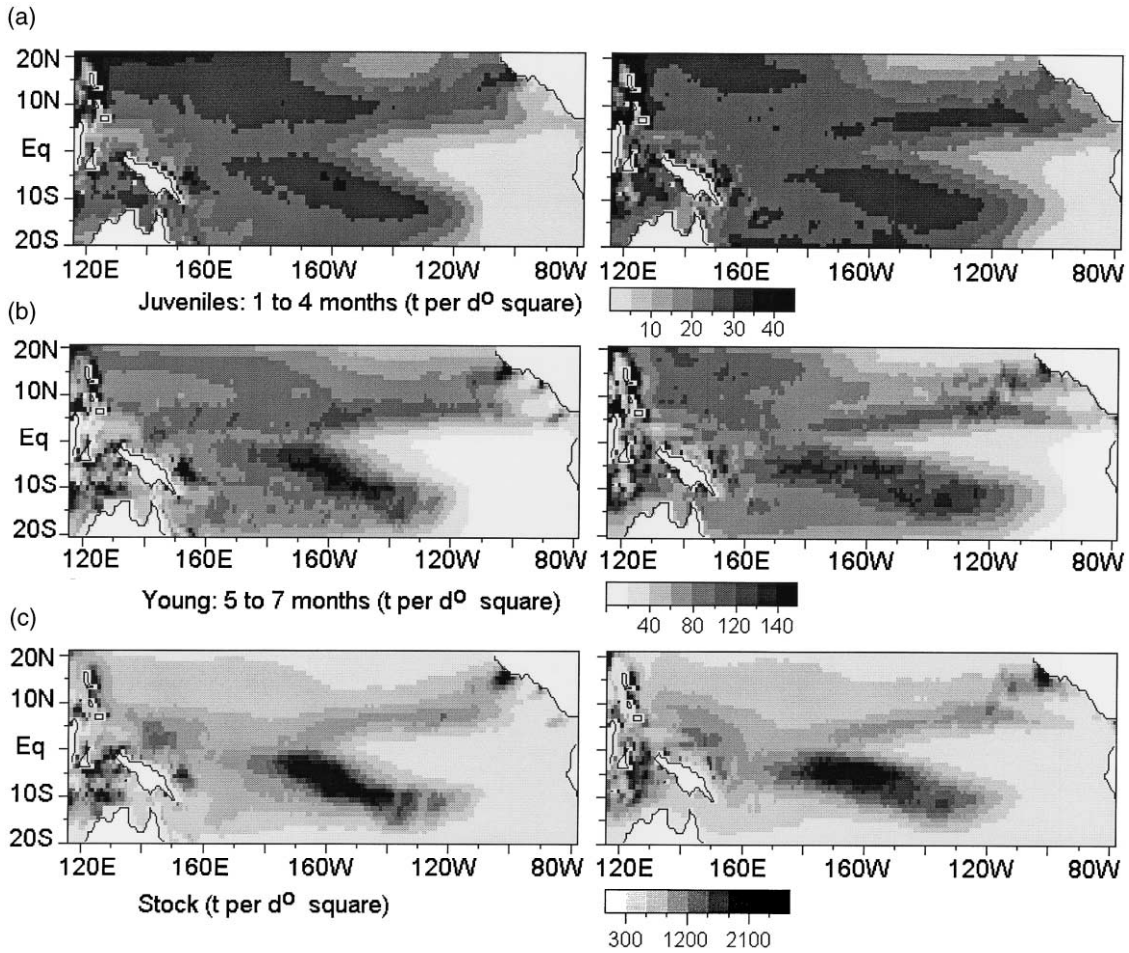

Fig. 8. Spatial distributions of larvae–juveniles (passive transport), young and virgin stock of skipjack for a mean situation in the 1st and 3rd quarter (1st quarter is the average of the 1st quarters of 1993, 1994 and 1995; 3rd quarter is the average of the 3rd quarters of 1992, 1993, and 1994).

an age of 4 months, when skipjack change from being passively advected to active movement enabling them to follow the increasing gradient of habitat index. The distribution of young skipjack (Fig. 8b) shows a transition between the large diffuse distribution of larvae and juveniles and the distribution of adults (stock) that concentrate in the zones of high habitat index (Fig. 8c).

9.3. Fisheries

Given the 20°N–20°S latitudinal range considered in the simulation, the spawning area delimited by the 26°C SST isotherm is almost totally covered. The recruitment level has been adjusted using an independent estimation from tagging experiment for the western Pacific stock (20°N–20°S, to 150°W) of 2–2.5.10^6 t (Kleiber et al., 1987). This leads to a total stock biomass of skipjack of ~3–3.5.10^6 t for the whole Pacific basin between 20°N and 20°S. The catchability coefficients for each fleet determined from this level of stock and the selectivity functions used, are given in Table 2. A low catchability coefficient for the eastern fishery is not surprising since this fleet is targeting yellowfin tuna. For the western fisheries, the catchability coefficient is very high for the Korean fleet, intermediate for the Japanese and Taiwan fleets and low for the US fleet. This is likely to result form bias in the predictions of the spatial distribution of the stock. The predicted concentration of fish may be too high in the central south equatorial region (where the US fleet is frequently fishing) but not high enough in the western Pacific (where the Korean fleet operates).

The total predicted monthly catch by each fleet is presented in Fig. 9. If the Philippine and Indonesian fleets are removed from the analysis because of the inaccuracies of their catch data, then the major inconsistency between observed and estimated catch comes from the US purse seine fleet. This fleet fishes furthest east in the WCPO and is, therefore, subject to the rapid fluctuations associated with ENSO events along the eastern edge of the warm pool. These rapid changes are unlikely to be reproduced with sufficient accuracy or occur as temporal or spatial shifts in the simulation. This feature will be useful to test further improvements of the model. A part of the catch in the eastern Pacific is missing because the simulated primary production did not encompass the coastal upwelling along the coasts of Peru and Chile. This biases the habitat index in this region, since the very high level of forage in this area along with the seasonal warming of water (Fig. 6) should produce a good habitat index that can be expected to attract skipjack at the beginning of the year. The predicted catch data for the other fleets agree rather well with the actual catch, considering the simplicity of the recruitment mechanisms in the model.

Since the population model is age-structured, it is possible to compare observed and predicted fish lengths in the catches (Fig. 10). Predicted length frequencies agree well with observations. However, the simulation cannot reproduce the fraction of the catch with the largest sizes. This is simply explained. The value of L_∞ used in the model is 70 cm, leaving unexplained the sizes range of 70–80 cm. The value of L_∞ is not the maximum size of skipjack, but a mean maximum size that does not reflect individual variability. Thus, the simulation indicates that the growth model used is not entirely satisfactory and could be improved. A second discrepancy concerns the fraction of small-sized fish that is usually larger in the simulation than in the observed catch. This may result from an inadequacy in the selectivity function. However, it should also be noted that observational data may well be biased because small fish are often discarded at sea to maintain space for the larger and more valuable fish, and so not get recorded in samples of landings.

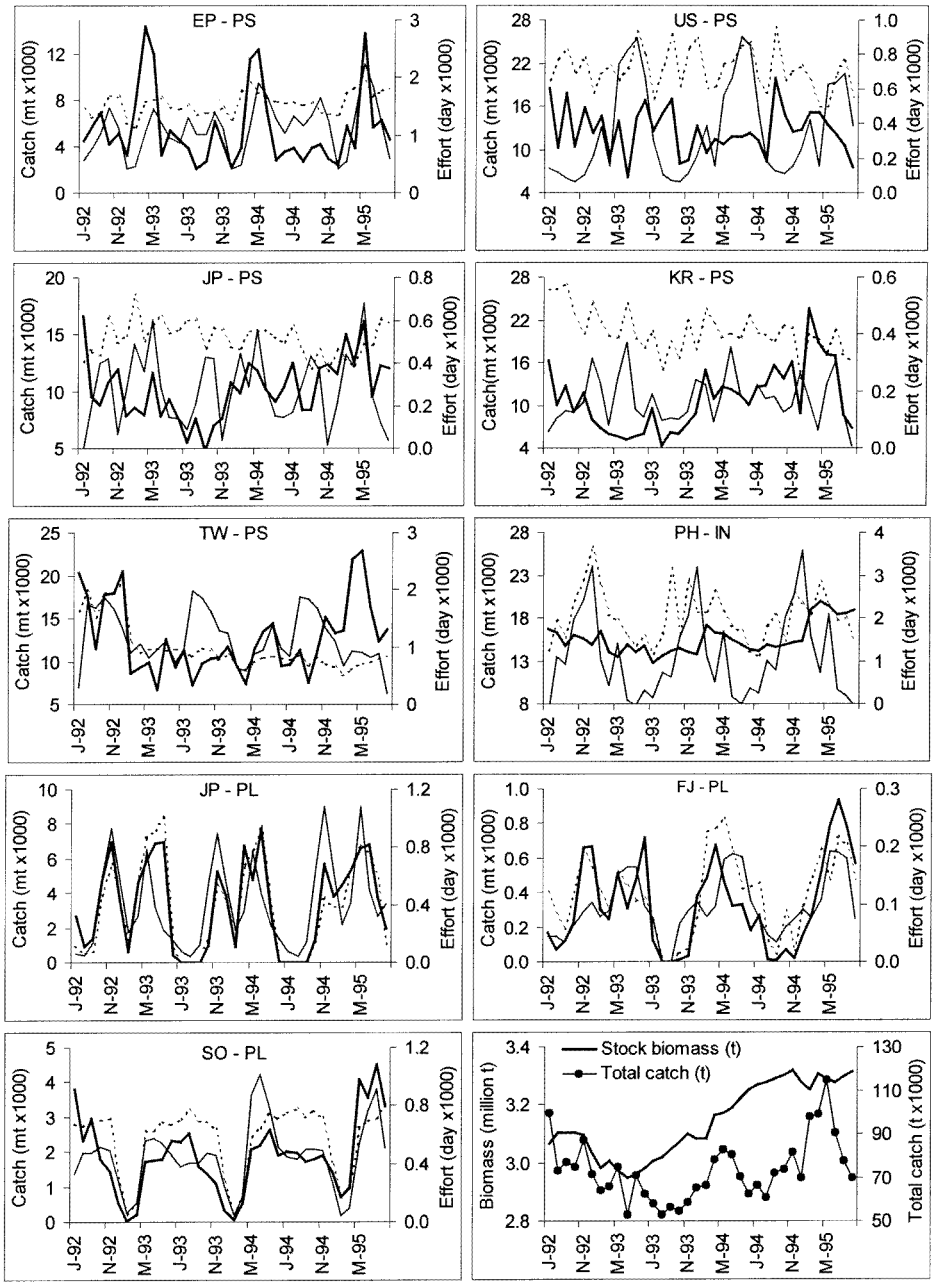

Fig. 9. Observed catch and effort and predicted catch of skipjack by fleet, and evolution of the predicted stock biomass. Thick line is predicted catch; thin line is observed catch; dotted line is effort (JP: Japan, KR: Korea, TW: Taiwan, US: United States of America, FJ: Fiji Islands, SO: Solomon Islands, PS: purse-seine, PL: pole-and-line, PH–IN: Philippine and Indonesia domestic fleets).

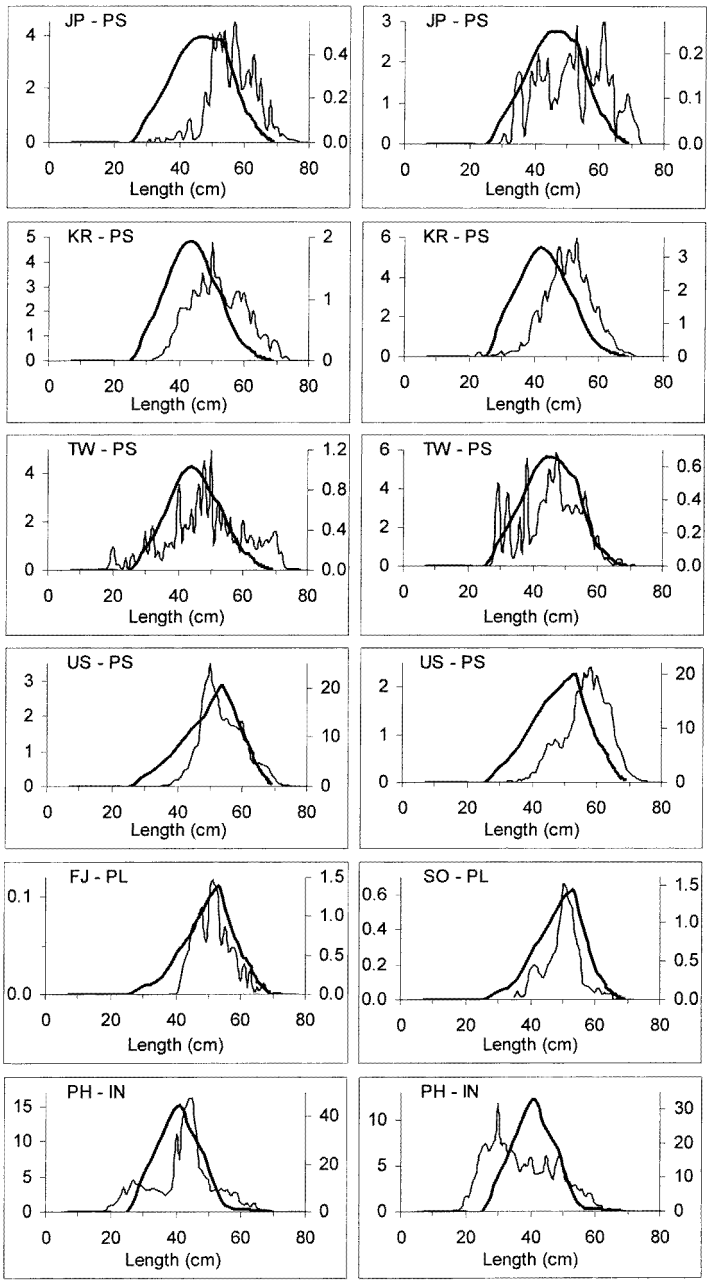

Fig. 10. Observed and predicted length frequencies for the skipjack catch by fleet during 1st (left) and 3rd (right) quarters. 1st quarter is the average of the 1st quarters of 1993, 1994 and 1995; 3rd quarter is the average of the 3rd quarters of 1992, 1993, and 1994. Thick line is predicted catch; thin line is observed catch (JP: Japan, KR: Korea, TW: Taiwan, US: United States of America, FJ: Fiji Islands, SO: Solomon Islands, PS: purse-seine, PL Pole-and-line, PH–IN: Philippine and Indonesia domestic fleets).

Finally, the spatial distribution of the observed and predicted total catch by the four main purse seine fleets is shown in Fig. 11. The mean coefficient of correlation between predicted and observed catch over the time series is 0.4. This is rather encouraging, given the high variability of observed catch at a one-degree square level, and the different limitations in the simulation. The catch east of 170°E appears to be the most difficult to predict in this simulation. As previously indicated, this is the region there is the largest variability as a result of the ENSO-related displacements of the eastern edge of the warm pool.

10. Discussion

The model SEPODYM described tries to integrate in the simplest possible way the knowledge of tuna biology and ecology. Model outputs constitute a management tool that allows for investigating environmental interactions and impacts on tuna stocks. Such an approach inevitably implies a switch from the single species model towards an ecosystem model, even if the ecosystem is drastically simplified. Nevertheless, it is a very flexible and useful tool, with multiple applications. Now that the overall structure of the model has been designed, many improvements can be envisaged.

The parameterization of the energy transfer through the ecosystem from primary productivity to the forage and finally to the tuna population requires more analyses to refine, test and validate the approach used in the model. This is particularly important since this first simulation indicates that the skipjack population is consuming ~20% of the total forage production, whereas a large

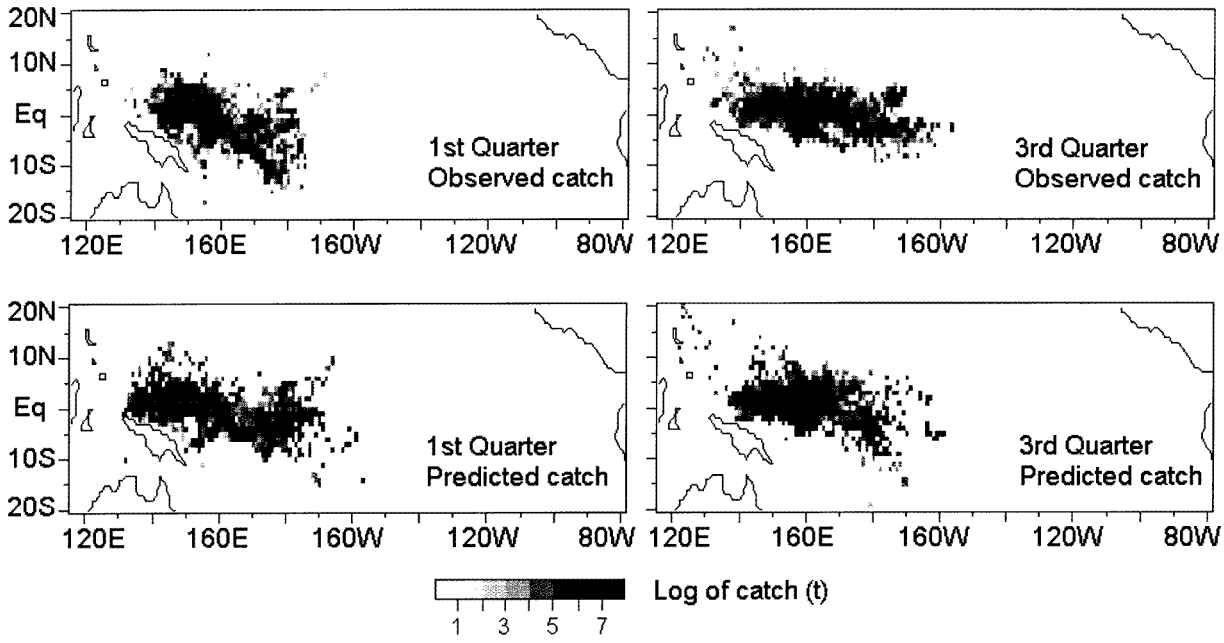

Fig. 11. Observed and predicted spatial distribution of the total catch by the four main purse-seine fleets (Japan, Korea, Taiwan, USA) for the 1st (R=0.40) and 3rd (R=0.67) quarters.

fraction of this production, e.g. mesopelagic fish, is not accessible to skipjack. It is also necessary to encompass the area of the whole tuna stock to reproduce the seasonal migrations toward subtropical waters, and to use longer time series including the most powerful ENSO events. Though important efforts have been devoted to the knowledge of skipjack biology, more research on this species is needed, particularly in defining growth. The model could easily integrate an 'individual variability' in growth that is linked to the environmental parameters (temperature, abundance of food). The population, fishery, and habitat parameterization could be improved with the help of statistical studies (generalized additive or linear models), individual based models (IBM) and statistical population dynamics models (e.g., MULTIFAN-CL, Fournier, Hampton, & Sibert, 1998).

Even with a simplified parameterization, this first simulation has been helpful in the interpretation of observed ENSO-related spatio-temporal changes in the distribution of skipjack population. Taken together, the results presented in this paper and the recent findings on the oceanography of the equatorial Pacific allow us to propose a conceptual model of the biological consequences of ENSO in the warm pool — cold tongue pelagic ecosystem (Fig. 12). During a normal situation, the cold tongue extends to 180°, and the well-developed equatorial divergence is the source of high primary productivity. In the western Pacific, the relatively low primary productivity of the mixed layer is associated with the presence of an atmospheric convective zone and a barrier layer. The equatorial divergence superimposed upon the mean westward zonal flux creates a spatial shift in the planktonic communities both on the meridional (poleward) and zonal (westward) axes.

With the development of El Niño, the system shifts eastward; the water masses of the warm pool extend towards the central Pacific while the intensity of the equatorial divergence decreases and the cold tongue retreats eastward. Secondary production, which previously had been developing in the cold tongue, moves into the warm pool, and eventually merges with secondary production originating in the western Pacific. Under the influence of currents, the organisms remain aggregated in a large zonal band associated with the convergent front along the eastern edge of the expanding warm pool. A longer residence time in the warm pool, clear waters and a physical subsurface barrier are all highly favorable to the feeding of surface tuna and this may explain the observed displacement of tuna populations linked to the movement of the convergence zone. As the atmospheric convective zone is displaced towards the central equatorial Pacific, a positive wind stress anomaly leads to the development of coastal upwelling along the north coast of Papua New Guinea, and more generally to an increase of primary production in the far western Pacific between Indonesia and 160°E–180°, according to the intensity of the event.

When eastward displacement of the system stops and starts to reverse, the eastern edge of the warm pool becomes less attractive. The westward displacement of the warm pool — cold tongue system limits the potential enrichment of surface waters of the eastern warm pool with the secondary production of the cold tongue. In addition, the decreased intensity of the equatorial divergence during El Niño is likely lead to a decrease in secondary productivity with a shift in time from a few weeks (zooplankton) to a few months (micronekton). On the other hand, the Papua New Guinea–Indonesian region that was enriched during the El Niño phase will have an increase in zooplankton and micronekton biomass at the time of the return to normal oceanographic conditions. Consequently, the attractiveness (in terms of tuna habitat) of the Papua New Guinea–Indonesian region should increase as it decreases at the eastern boundary of the warm pool. This situation could explain the westward movement of tagged tuna observed during this phase

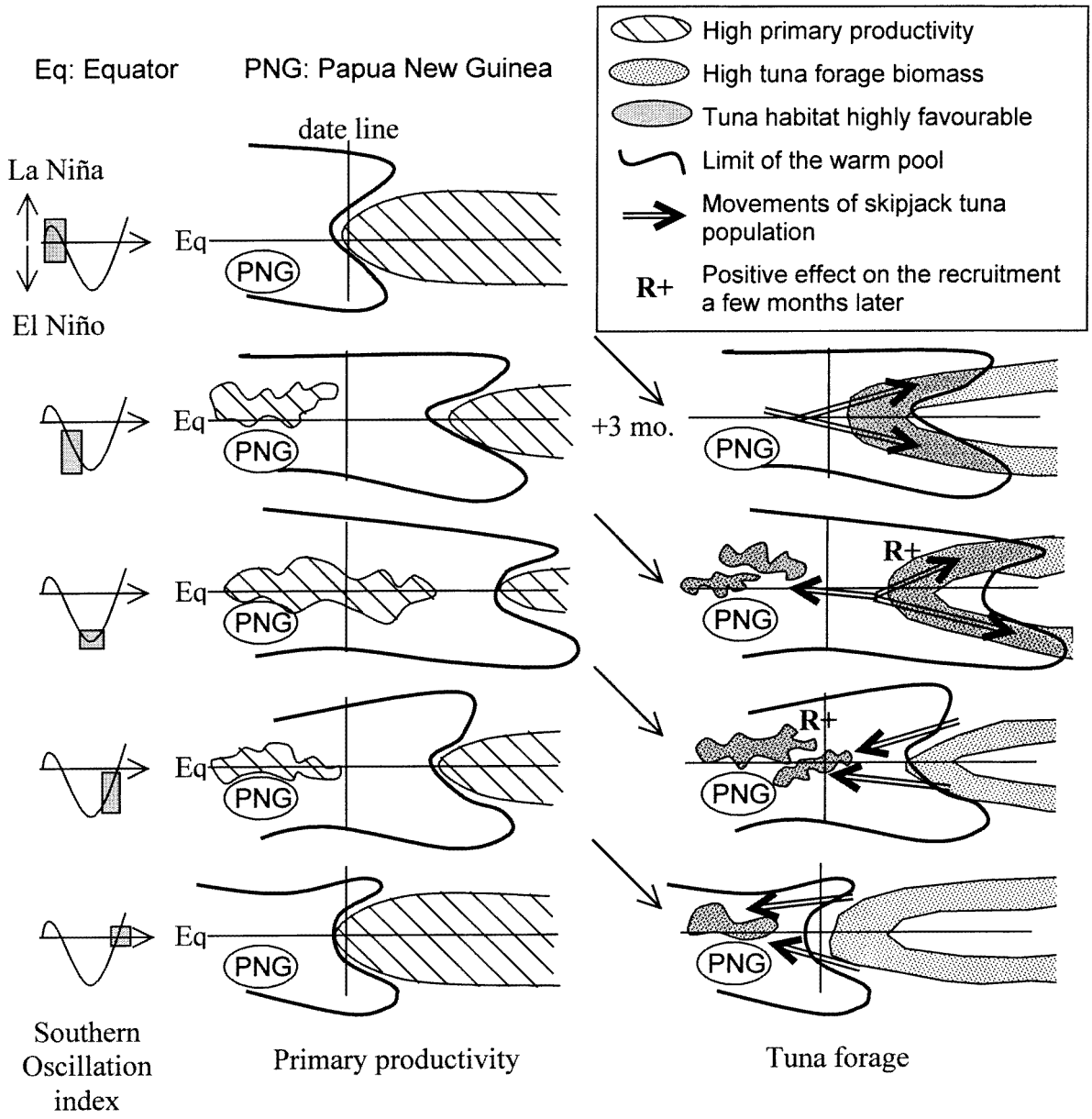

Fig. 12. Schematic diagram of the biological consequences of the development of an El Niño event in the pelagic ecosystem for the equatorial western and central Pacific ocean (the lag between each step is approximately three months). During a mean situation, there is a well developed cold tongue in the central Pacific with a high level of primary production, while the western Pacific is characterized by the presence of the atmospheric convective zone and general low primary productivity. The equatorial divergence within a mean westward zonal flux creates a spatial shift in the planktonic communities both on the meridional and zonal axes. When the system shifts eastward (El Niño) an important biomass of forage becomes accessible to tuna predation in the oceanic convergence zone of the warm pool — cold tongue system. The eastward displacement of the atmospheric convective zone is associated to the shift or vanishing of the barrier layer and stronger wind stresses than usual in the western region, leading to an increase of primary production. When the displacement is reversed, the eastern edge of the warm pool becomes less attractive, but the western region has developed an increased zooplankton and micronekton biomass, increasing the attractiveness and possibly explaining the rapid westward movement of tuna observed during this phase as well as a high level of recruitment.

(Lehodey et al., 1997). The probable enrichment in zooplankton of the western Pacific during the El Niño phase is a condition highly favorable for survival and larval development of the tuna. Such conditions might therefore be expected to produce strong tuna recruitment to the fisheries six to twelve months later. Preliminary investigations (Lehodey, 2000) seem to confirm that El Niño events eventually have a favorable impact on skipjack recruitment in the western Pacific, and the model SEPODYM is an ideal tool for analyzing these mechanisms.

In summary, the western Pacific warm pool displays remarkable dynamic in biological productivity, balancing the 'Papua New Guinea–Indonesian' region and the warm pool-cold tongue convergence zone in an out-of-phase pattern. By contrast, in the eastern Pacific, primary production and 'down-stream' tuna forage are high and stable in space and time, except during the most powerful El Niño events. From a skipjack habitat point of view, the lower but sufficient secondary production of the warm pool compared to the eastern Pacific is likely compensated by better environmental conditions in terms of temperature, oxygen, and water clarity. In the eastern Pacific, the high forage level is probably tempered by sub-optimal values of other environmental parameters. While El Niño events have catastrophic consequences in the eastern Pacific, it appears that they have beneficial impacts on the biological productivity in the western equatorial Pacific.

Acknowledgements

I am grateful to colleagues who provided the data used in the present study: particularly the NASA/GSFC Distributed Active Archive Center, for the CZCS and SeaWiFS satellite-derived data of phytoplankton pigment concentration, and all the colleagues at LODYC, P. Delecluse and her team, A. Stoens, Y. Dandonneau, L. Memery, C. Menkes, M.-H. Radenac and J.-M. André for the data of the OPA OGCM and the coupled biogeochemical outputs of primary production. Many thanks also to T. Delcroix, R. Grandperrin at IRD in Noumea and to my colleagues T. Lewis, J. Hampton, and K. Bigelow, for their helpful comments and revision of a first manuscript. A very special thanks to M. Bertignac who developed the first version of the spatial tuna dynamic model. This work was supported by the European Union-funded South Pacific Regional Tuna Resource Assessment and Monitoring Project of the Oceanic Fisheries Programme of the Secretariat of the Pacific Community.

Appendix A. Description of the main symbols used in SEPODYM

Symbol	Description	Unit
P	New primary production	mmol N d^{-1} m^{-2}
S	Recruitment in the forage population	mmol N d^{-1} m^{-2}
F'	Forage production (=S if S constant)	mmol N d^{-1} m^{-2}
F	Forage biomass	mmol N m^{-2}
T_r	Time of recruitment in the forage population	d
E	N transfer efficiency from P to S (0.04)	
m_r	(=$-\mathrm{Ln}(E)/T_r$) Loss rate from P to S, assuming an exponential decreasing function during T_r	d^{-1}

λ	Total mortality rate of forage	d^{-1}
c_1	Ratio of fish C/N (3.6)*	
c_2	Ratio of fish dry weight to C (2.4)*	
c_3	Ratio of fish wet weight to dry weight (3.3)*	
c_4	Conversion coefficient from Mmol N to wet weight (g) of fish ($c_1.c_2.c_3.15.10^{-3}$=0.428)	
λ'	Residual mortality rate of forage	d^{-1}
ω	Specific mortality rate of forage due to predator (tuna) species	d^{-1}
u	Zonal term of current	Nm d^{-1}
v	Meridional term of current	Nm d^{-1}
ρ	Diffusion coefficient for the forage	Nm^2 d^{-1}
N	Number of individuals in the tuna population	
R	Recruitment in tuna population	$month^{-1}$
Z	Total mortality rate of tuna population	$month^{-1}$
M	Natural mortality of tuna population	$month^{-1}$
f	Fishing mortality rate of tuna population	$month^{-1}$
w	Weight of tuna	kg
s	Selectivity coefficient of the fishing gear	
q	Catchability coefficient of the fleet	
J	Fishing effort	d
C	Tuna catch	mt (metric tonnes)
σ	Standard error for the temperature function	
θ	Mean value of the temperature function	°C
H	Habitat index	
I	Forage index	
r	Daily ration relative to the body weight	
X_o	Advection coefficient for tuna movement (~viscosity coefficient in MacCall (1990) acceptation)	
D	Diffusion coefficient for tuna species	Nm^2 d^{-1}

*(Vinogradov, 1953 in Iverson, 1990)

References

Allen, K. R. (1971). Relation between production and biomass. *Journal of the Fisheries Research Board of Canada*, *28*, 1573–1581.

Barkley, R. A., Neill, W. H., & Gooding, R. M. (1978). Skipjack tuna (*Katsuwonus pelamis*) habitat based on temperature and oxygen requirements. *Fishery Bulletin*, *76*, 653–662.

Bertignac, M., Lehodey, P., & Hampton, J. (1998). A spatial population dynamics simulation model of tropical tunas using a habitat index based on environmental parameters. *Fisheries Oceanography*, *7*, 326–335.

Bills, P. J., & Sibert, J. R. (1997). Design of tag–recapture experiments for estimating yellowfin tuna stock dynamics, mortality, and fishery interactions. University of Hawaii, Joint Institute for Marine and Atmospheric Research. JIMAR Contribution 97, 1–80.

Blanke, B., & Delecluse, P. (1993). Variability of the tropical Atlantic Ocean simulated by a general circulation model with two different mixed-layer physics. *Journal of Physical Oceanography*, *23*, 1363–1388.

Borgmann, U. (1982). Particle-size conversion efficiency and total animal production in pelagic ecosystems. *Canadian Journal of Fishery and Aquatic Sciences*, *40*, 2010–2018.

Borgmann, U. (1987). Models on the slope of, and biomass flow up, the biomass size spectrum. *Canadian Journal of Fishery and Aquatic Sciences*, *44*, 136–140.

Boudreau, P. R., & Dickie, L. M. (1989). Biological model of fisheries production based on physiological ecological scalings of body size. *Canadian Journal of Fishery and Aquatic Sciences*, *46*, 614–623.

Boudreau, P. R., & Dickie, L. M. (1992). Biomass spectra of aquatic ecosystems in relation to fisheries yield. *Canadian Journal of Fishery and Aquatic Sciences*, *49*, 1528–1538.

Brill, R. W. (1994). A review of temperature and oxygen tolerance studies of tunas pertinent to fisheries oceanography, movement models and stock assessments. *Fisheries Oceanography*, *3*, 204–216.

Cousins, S. H. (1985). The trophic continuum in marine ecosystems: structure and equations for a predictive model. In R. E. Ulanowicz, & T. Platt (Eds.), *Ecosystem theory for biological oceanography*. *Canadian Bulletin of Fishery and Aquatic Sciences*, *213*, 76–93.

Cushing, D. H. (1995). The long-term relationship between zooplankton and fish. *ICES Journal of Marine Sciences*, *52*, 611–626.

Dalzell, P. J. (1993). Small pelagic fishes. In A. Wright, & L. Hill, *Nearshore marine resources of the South Pacific* (pp. 97–133). Canada: IPS, Suva, FFA, Honiara, ICOD.

Delcroix, T. (1998). Observed surface oceanic and atmospheric variability in the tropical Pacific at seasonal and ENSO time-scales: a tentative overview. *Journal of Geophysical Research*, *103*, 18611–18633.

Delcroix, T., Eldin, G., & Radenac, M.-H. (1992). Variation of the western equatorial Pacific Ocean, 1986–1988. *Journal of Geophysical Research*, *97*, 5423–5445.

Dickie, L. M., Kerr, S. R., & Schwinghamer, P. (1987). An ecological approach to fisheries assessment. *Canadian Journal of Fishery and Aquatic Sciences*, *44*, 68–74.

Forsbergh, E. D. (1980). Synopsis of biological data on the skipjack tuna, *Katsuwonus pelamis*, (Linnaeus, 1758), in the Pacific Ocean. *IATTC. Spec. Rep.*, *2*, 295–360.

Fournier, D. A., Hampton, J., & Sibert, J. R. (1998). MULTIFAN-CL: a length-based, age-structured model for fisheries stock assessment, with application to South Pacific albacore, *Thunnus alalunga*. *Canadian Journal of Fishery and Aquatic Sciences*, *55*, 2105–2116.

France, R., Chandler, M., & Peters, R. (1998). Mapping trophic continua of benthic foodwebs: body size — δ^{15}N relationships. *Marine Ecology Progress Series*, *174*, 301–306.

Fretwell, S. (1972). *Population in a seasonal environment.* New Jersey: Princeton University Press 217 pp.

Fretwell, S., & Lucas, H. (1970). On the territorial behaviour an other factors influencing habitat distribution in birds. *Acta Biotheoretica*, *19*, 16–36.

Gomez-Gutierrez, J., & Sanchez-Ortiz, C. A. (1997). Larval drift and population structure of the pelagic phase of *Pleuroncodes planipes* (Stimpson) (Crustacea:Galatheidae) off the southwest coast of Baja California, Mexico. *Bulletin of Marine Science*, *61*, 305–325.

Hida, T. S. (1973). Food of tunas and dolphins (Pisces: Scombridae and Cryphaenidae) with emphasis on the distribution and biology of their prey *Stolephorus buccaneeri* (Engraulidae). *Fishery Bulletin U.S.*, *71*, 135–143.

Isaacs, J. D. (1977). The life of the open sea. *Nature, London*, *267*, 778–780.

Iverson, R. L. (1990). Control of marine fish production. *Limnology Oceanography*, *35*, 1593–1604.

Jackson, G. D., & Choat, J. H. (1992). Growth in tropical cephalopods: an analysis based on statolith microstructure. *Canadian Journal of Fishery and Aquatic Sciences*, *49*, 218–228.

Kerr, S. R. (1974). Theory of size distribution in ecological communities. *Journal of the Fisheries Research Board of Canada*, *31*, 1859–1862.

Kitchell, J. F., Boggs, C., He, X., & Walters, C. J. (1999). Keystone predators in the Central Pacific. In *Ecosystem approaches for fisheries management* (pp. 665–683). The Lowell Wakefield Symposium Series. Alaska Sea Grant College Program, Fairbanks, Alaska.

Kleiber, P., Argue, A. W., & Kearney, R. E. (1987). Assessment of Pacific skipjack tuna (*Katsuwonus pelamis*) resources by estimating standing stock and components of population turnover from tagging data. *Canadian Journal of Fishery and Aquatic Sciences*, *44*, 1122–1134.

Lehodey, P. (2000). Impacts of the El Niño Southern Oscillation on tuna populations and fisheries in the tropical Pacific

Ocean. Oceanic Fisheries Programme. Noumea, New Caledonia, Secretariat of the Pacific Community. Working Paper. RG-1 1–32.
Lehodey, P., Andre, J.-M., Bertignac, M., Hampton, J., Stoens, A., Menkes, C., Memery, L., & Grima, N. (1998). Predicting skipjack tuna forage distributions in the equatorial Pacific using a coupled dynamical bio-geochemical model. *Fisheries Oceanography*, *7*, 317–325.
Lehodey, P., Bertignac, M., Hampton, J., Lewis, A., & Picaut, J. (1997). El Nino Southern Oscillation and tuna in the western Pacific. *Nature, London*, *389*, 715–718.
Longhurst, A. R., Sathyendranath, S., Platt, T., & Caverhill, C. (1995). An estimate of global primary production in the ocean from satellite radiometer data. *Journal of Plankton Research*, *17*, 1245–1271.
Lukas, R., & Lindström, E. (1991). The mixed layer of the western equatorial Pacific Ocean. *Journal of Geophysical Research*, *96*, 3343–3457.
Magnuson, J. J., & Heitz, J. G. (1971). Gill raker apparatus and food selectivity among mackerels, tunas, and dolphins. *Fishery Bulletin*, *69*, 361–369.
Matsumoto, W. M., Skillman, R. A., & Dizon, A. E. (1984). Synopsis of biological data on skipjack tuna, *Katsuwonus pelamis*. *NOAA Technical Report, National Marine Fishery Sciences*, *451*, 1–92.
MacCall, A. D. (1990). *Dynamic geography of marine fish population*. Books in recruitment fishery oceanography, University of Washington Press, 153 pp.
MacPhaden, M. J., & Picaut, J. (1990). El Niño–Southern Oscillation Index displacements of the Western Equatorial Pacific wrm pol. *Science*, *50*, 1385–1388.
Mori, K. (1972). Geographical distribution and relative apparent abundance of some scombrid fishes based on the occurrences in the stomachs of apex predators caught on tuna longline — I. Juvenile and young of skipjack tuna (*Katsuwonus pelamis*). *Bulletin of the Far Seas Fisheries Research Laboratory*, *6*, 111–157.
Murray, J. D. (1993). *Mathematical biology*. In S. A. Levin (Ed.), *Biomathematics*. Berlin, Heidelberg, New York, *19*, 767 pp.
Murtugudde, R. G., Signorini, S. R., Christian, J. R., Busalacchi, A. J., McClain, C. R., & Picaut, J. (1999). Ocean color variability of the tropical Indo-Pacific Basin observed by SeaWiFS during 1997–1998. *Journal of Geophysical Research*, *104*, 18351–18366.
Nishikawa, Y., Honma, M., Ueyanagi, S., & Kikawa, S. (1985). Average distribution of larvae of oceanic species of scombroid fishes, 1956–1981. *Far Seas Fishery Research Laboratory. S Series*, *12*, 1–99.
Okubo, A. (1980). *Diffusion and ecological problems: mathematical models*. Springer-Verlag, New York, 254 pp.
Okubo, A. (1986). Dynamical aspects of animal grouping: swarms, schools, flocks, and herds. *Advanced Biophysics*, *22*, 1–94.
Picaut, J., & Delcroix, T. (1995). Equatorial wave sequence associated with warm pool displacements during the 1986–89 El Niño–La Niña. *Journal of Geophysical Research*, *100*, 18393–18408.
Picaut, J., Masia, F., & Du Penhoat, Y. (1997). An advective–reflective conceptual model for the oscillatory nature of the ENSO. *Science*, *277*, 663–666.
Platt, T. (1985). Structure of the marine ecosystem: its allometric basis. In R. E. Ulanowicz, & T. Platt, *Ecosystem theory for biological oceanography* (pp. 55–64).
Press, W. H., Teukolsky, S. A., Vetterling, W. T., & Flannery, B. P. (1992). *Numerical recipes in C. The art of scientific computing*. Cambridge: Cambridge University Press 1-994.
Rodriguez, J., & Mullin, M. M. (1986). Relation between biomass and body weight of plankton in a steady state oceanic ecosystem. *Limnology Oceanography*, *21*, 361–370.
Roger, C. (1971). *Les euphausiacés du Pacifique equatorial et sud tropical*. Thèse de doctorat, Université de Provence — ORSTOM, 331 pp.
Schaefer, K. M. (1998) Reproductive biology of yellowfin tuna (*Thunnus albacares*) in the eastern Pacific Ocean. Bayliff, W. H. La Jolla, California, USA, Inter-American Tropical Tuna Commission. *Bulletin*, *21*, 205–272.
Sharp, G. D., & Dizon, A. E. (1978). *The physiological ecology of tunas.* New York: Academic Press, 485 pp.
Sheldon, R. W., Prakash, A., & Sutcliffe Jr, W. H. (1972). The size distribution of particles in the Ocean. *Limnology Oceanography*, *17*, 327–340.
Sheldon, R. W., Sutcliffe, W. H. Jr., & Paranjape, M. A. (1977). Structure of pelagic food chain and relationship between plankton and fish production. *Journal of the Fisheries Research Board of Canada*, *34*, 2344–2353.

Shushkina, E. A., Vinogradov, M. E., Lebedeva, L. P., & Anokhina, L. L. (1997). Productivity characteristics of epipelagic communities of the World's Oceans. *Oceanology*, *37*, 346–353.

Shushkina, E. A., Vinogradov, M. E., Sheberstov, S. V., Nezlin, N. P., & Gagarin, V. I. (1996). Characterization of epipelagic ecosystems of the Pacific Ocean on the basis of the satellite and field observations: the plankton stock in the epipelagial. *Oceanology*, *35*, 643–649.

Sibert, J. R., Hampton, J., Fournier, D. A., & Bills, P. J. (1999). An advection-diffusion–reaction model for the estimation of fish movement parameters from tagging data, with application to skipjack tuna (*Katsuwonus pelamis*). *Canadian Journal of Fishery and Aquatic Sciences*, *56*, 925–938.

Sibert, J. R., & Fournier, D. A. (1994). Evaluation of advection–diffusion equations for estimation of movement patterns from tag recapture data. In R. S. Shomura, J. Majkowski, & S. Langi (Eds.), *Interactions of Pacific tuna fisheries* (pp. 108–121). Rome: FAO Fisheries Technical Papers. FAO.

Silvert, W., & Platt, T. (1978). Energy flux in the pelagic ecosystem: a time-dependent equation. *Limnology Oceanography*, *23*, 813–816.

Skellam, J. G. (1973). The formulation and interpretation of mathematical models of diffusional process in population biology. In Bartlett, M. S., & Hiorns, R. W. (Eds.), *The mathematical theory of the dynamic of biological populations* (pp. 63–85). New York.

Stoens, A., Menkes, C., Dandonneau, Y., & Memery, L. (1998). New production in the equatorial Pacific: a coupled dynamical–biogeochemical model. *Fisheries Oceanography*, *7*, 311–316.

Stoens, A., Menkes, C., Radenac, M.-H., Dandonneau, Y., Grima, N., Eldin, G., Memery, L., Navarette, C., Andre, J.-M., Moutin, T., & Raimbault, P. (1999). The coupled physical-new production system in the equatorial Pacific during the 1992–95 El Niño. *Journal of Geophysical Research*, *104*, 3323–3339.

Ueyanagi, S. (1969). Observations on the distribution of tuna larvae in the Indo-Pacific Ocean with emphasis on the delineation of the spawning areas of Albacore, *Thunnus alalunga*. *Bulletin of the Far Seas Fisheries Research Laboratory*, *2*, 177–215.

Vialard, J., & Delecluse, P. (1998). An OGCM study for the TOGA decade. Part I: role of salinity in the physics of the western Pacific fresh pool. *Journal of Physical Oceanography*, *28*, 1071–1088.